

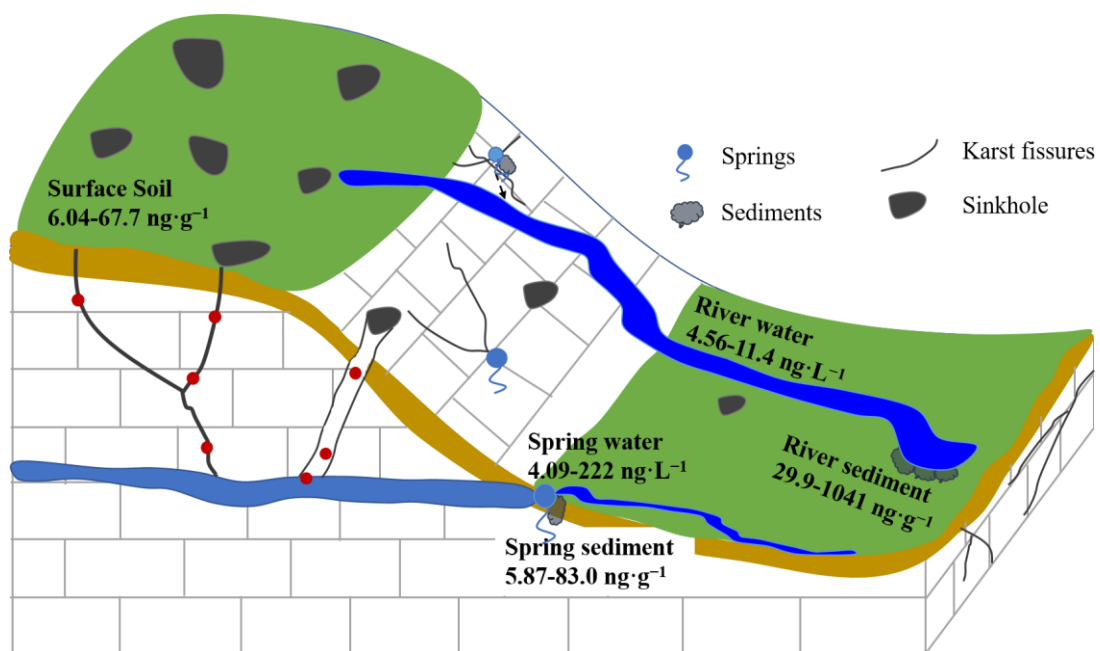


28 **HIGHLIGHTS**

- 29 ➤ Particle-promoted transport with rapid water flow was pivotal for PAHs
- 30 mobilization to sediments.
- 31 ➤ Different sources and matrix components lead to the differences in PAHs
- 32 concentrations and compositions in river sediments and spring sediments.
- 33 ➤ Coal combustion, biomass burning and vehicle emission account for 99.1% of
- 34 sources of the total PAHs.
- 35 ➤ Significant correlations of PAHs compositions were observed in the multimedia
- 36 environment of karst spring systems.

37

38 **TOC**



39

40

41 **ABSTRACT**

42 Karst groundwater is an important water resource but it is vulnerable to contaminants,  
43 due to the distinctive geological features of abundant transmissive fractures and  
44 conduits which connect the surface to the underground system. Anthropogenic activity-  
45 derived polycyclic aromatic hydrocarbons (PAHs) on the surface environment could  
46 enter groundwater easily and rapidly and threaten water security in karst areas. Samples  
47 in the multimedia environment from 10 specific karst spring systems from Western  
48 Hubei of Central China were collected to analyze 16 priority PAHs and to investigate  
49 their transport in these karst spring systems. The total concentrations of PAHs in the  
50 soil, river water, river sediments, spring water, and spring sediments ranged between  
51 6.04 and 67.7 ng·g<sup>-1</sup>, 4.56 and 11.4 ng·L<sup>-1</sup>, 29.9 and 1041 ng·g<sup>-1</sup>, 4.09 and 222 ng·L<sup>-1</sup>,  
52 and 5.88 and 83.0 ng·g<sup>-1</sup>, respectively. Levels of PAHs in this area were relatively low  
53 when compared to other karst areas. Proportions of low-molecular-weight (LMW)-  
54 PAHs in the water, sediments and soil (average 58.2-78.8%) were much higher than  
55 those of high-molecular-weight (HMW)-PAHs. The proportion of LMW-PAHs in the  
56 sediments (especially in river sediments) was higher than that in the soil. Characteristic  
57 ratios analysis and principal component analysis showed that PAHs were from high-  
58 temperature combustion of the mixture of coal and biomass, and vehicle emission,  
59 where coal and biomass combustion are the dominant sources. Significant correlations  
60 of PAHs compositions in different media of karst spring systems were observed,  
61 especially in the Yuquangdong (YQD), Jiuzhenziquan (JZZQ), Xianyudong (XYD) and  
62 Fengdong (FD) karst spring systems, indicating the rapid PAH transport from the  
63 recharge area soil to the discharge area of spring water and sediments.

64

65 **Keywords:** Karst spring, Polycyclic aromatic hydrocarbons (PAHs), Transport,  
66 Source analysis, Hydrogeological conditions, Western Hubei

## 67 1. INTRODUCTION

68 Polycyclic aromatic hydrocarbons (PAHs) are widespread in the multimedia  
69 environment; they are persistent, toxic, carcinogenic and mutagenic (Niu et al. 2017,  
70 Qu et al. 2019). PAHs mainly originate from incomplete combustion of fuels, such as  
71 petroleum, coal and biomass, and other fossil fuels. They are combustion-derived and  
72 semi-volatile, and therefore are easily to enter the atmosphere. PAHs in the atmosphere  
73 can enter the topsoil through dry or wet depositions and are then transported to the  
74 surface and groundwater systems by surface runoff and infiltration (Guo et al. 2009,  
75 Ligaray et al. 2016, Maliszewska - Kordybach et al. 2007, Zhu et al. 2015), and  
76 threaten the hydro-ecosystem and human health.

77 Karst systems are particularly vulnerable to contaminants due to their unique  
78 hydrogeological features. Contaminants can easily infiltrate through the thin and  
79 scattered karst soil layer or pass through the sinkholes and fissures (Zhang et al. 2017),  
80 and be transported from the surface to groundwater systems (Huang et al. 2021, Qian  
81 et al. 2020, Zeng et al. 2018). Karst spring water can provide abundant high-quality  
82 groundwater as drinking water and agricultural water for local residents. Once the  
83 groundwater is polluted, it will directly affect people's domestic water, livestock water  
84 and farmland irrigation in the karst region. Therefore, studying the pollution transport  
85 processes in karst spring systems has important scientific significance, especially for  
86 typical pollutants, such as PAHs. At the same time, in order to protect human and  
87 ecosystem health, it is vital to monitor contaminants in the karst springs.

88 Some studies have reported the environmental behaviors and characteristics of  
89 PAHs in karst systems. Simmleit and Herrmann (1987) found that PAHs transport in  
90 the karst aquifer mainly depends on their physical-chemical properties. Schwarz et al.  
91 (2011) observed that PAHs usually accumulated in soils only, even in the highly-  
92 vulnerable karst area. Some scholars investigated the PAHs pollution in surface water  
93 and soil in karst area (Levy et al. 2017, Ligaray et al. 2016, Maioli et al. 2011, Moeckel  
94 et al. 2014), and conducted ecological risk assessment (ERA) of PAHs in these karst

95 areas (Lan et al. 2019, Sun et al. 2020).

96        However, to the best of our knowledge, few studies have focused on PAH  
97 contamination in both the surface and underground of the whole karst spring systems.  
98 Studying pollution only in the surface systems fails in capturing the potential transport  
99 of PAHs to groundwater. Since the surface system is connected with the underground  
100 system, especially in karst areas with thin and uneven soil and highly-developed  
101 fissures and conduits. Combining research of both surface and underground systems is  
102 helpful to understand the sources of groundwater pollution and the transport of PAHs  
103 in the karst systems, to help protect groundwater resources in the karst areas. Thus, the  
104 complete karst spring systems, including the recharge area soil, spring water and spring  
105 sediment, and the spring-discharged surface water and surface sediment, were  
106 considered as whole units in this study. The purposes of this study were therefore: 1) to  
107 determine the concentrations, compositions and distribution characteristics of PAHs in  
108 the multimedia environment in the rural karst area in western Hubei of Central China,  
109 2) to diagnose the sources of PAHs in the study karst area and 3) to analyze the transport  
110 process and characteristics of PAHs in karst spring systems with different  
111 hydrogeological and hydrodynamic conditions.

## 112 **2. MATERIALS AND METHODS**

### 113 **2.1 Research area and sampling**

114        The study area is located on the south bank of the Yangtze River in Yichang,  
115 Central China (**Figure 1**). Carbonates from Sinian to Triassic are wide-distributed  
116 regionally. Due to the proper climate condition, karst geomorphology is well-developed.  
117 It belongs to the karst trough zone of China, with a large number of middle-low  
118 mountains and deep valleys (Liu et al. 2020). In this area, numerous sinkholes and  
119 grooves develop on the up-platform and large springs are generated at the bottom of  
120 valleys, and the relative height difference is between 500-1200m. Precipitation is the

121 main water source here. It can infiltrate through soil and small fissures slowly, and it  
122 also can converge into sinkholes in karst depressions and troughs rapidly. For the  
123 decentralized infiltration recharge, the groundwater is often discharged dominantly by  
124 karst fissure network and then flows into karst conduits or directly to the outlets, which  
125 is relatively slow. While for the concentrated recharge, the groundwater flows directly  
126 into conduits, which contributes to the peak flows greatly. Generally, underground  
127 rivers and big springs distribute at the bottoms of deep gullies and canyons, while  
128 smaller springs scattered distributes in valleys and gullies.

129 It has a subtropical monsoon climate in the study area. The average annual rainfall  
130 is ca. 1440 mm and concentrates during the period from May to August. The primary  
131 water sources of springs are atmospheric precipitation and karst groundwater. The study  
132 area is located in a rural area, including agricultural and residential areas. Due to the  
133 unique hydrogeological condition of karst, impacts from agricultural activity and rural  
134 residences in the significant depressions on the up-platform are the primary pollution  
135 sources of springs. Pollutants could easily be transported with soil particles by the  
136 rainfall and runoff with the rapid water flow to springs.

137 Totally ten typical spring systems, namely Zhoupinglongdong (ZPLD), Dayuquan  
138 (DYQ), Migongquan (MGQ), Yuquandong (YQD), Xianyudong (XYD),  
139 Xiachangchong (XCC), Jiuzhenziqian (JZZQ), Wuzhuaquan (WZQ), Chaoshuidong  
140 (CSD) and Fengdong (FD), were selected for sampling in October 2019 after intensive  
141 agriculture activity to avoid the impact of ploughing and fertilizing. Generally, spring  
142 water, spring sediments and soils from surrounding farmland were collected (**Figure 1**)  
143 for each spring, including 10 spring water (SW) samples, 8 spring sediment (SS)  
144 samples, 9 surface soil (S) samples (5 around spring outlets and 4 from spring recharge  
145 area), 10 river water (RW) samples and 10 river sediments (RS) samples.

146 Water samples were collected into 2 L amber glass bottles at the spring outlets  
147 (SW) and in the rivers (RW). Sediment samples were collected from the spring outlets  
148 (SS) and in the rivers downstream of the springs (RS). Surface soil samples (S) were

149 collected from the surface layer (0-20 cm) of farmland. Solid samples (sediments and  
 150 soils) were collected by a stainless-steel shovel. Each soil sample (ca. 1 kg) was  
 151 collected and mixed from three to five sub-samples within a 100 m<sup>2</sup> area. The solid  
 152 samples were wrapped into the aluminum foil and sealed in polyethylene zip bags. The  
 153 samples were temporarily stored in a car-cooler (ca. 4 °C) during the sampling  
 154 campaign and transportation. Afterwards they were delivered to the State Key  
 155 Laboratory of Biogeology and Environmental Geology (Wuhan, China), water samples  
 156 were stored in a refrigerator (4 °C) before being pretreated within a week. Solid samples  
 157 were freeze-dried, ground to pass through the 100-mesh sieve, and kept in the freezer  
 158 (-20 °C) before pretreatment.



159

160 **Figure 1.** Sketch map of the karst study area and sampling sites in the spring systems

## 161 2.2 Sample pretreatment and PAHs analysis

162 Samples was pretreated and analyzed in the State Key Laboratory of Biogeology  
163 and Environmental Geology in Wuhan, China. The pretreatment procedures of water,  
164 sediments and soil samples followed the description in the previous study from the same  
165 research group (Xing et al. 2016) with minor modification. Briefly, each water sample  
166 (2 L) was spiked with 5.0  $\mu\text{L}$  of recovery surrogates ( $200 \text{ mg L}^{-1}$ , a mixture solution  
167 including five deuterated PAH compounds, namely Naphthalene-D<sub>8</sub>, Acenaphthene-  
168 D<sub>10</sub>, Phenanthrene-D<sub>10</sub>, Chrysene-D<sub>12</sub>, and Perylene-D<sub>10</sub>, purchased from Dr.  
169 Ehrenstorfer, Germany). Each water sample was then extracted by liquid-liquid  
170 extraction (LLE) in a separation funnel. Dichloromethane (DCM, gas chromatography  
171 (GC) grade, purchased from Tedia, USA) was added 3 times to extract PAHs. The  
172 extract was then stored in a flask with anhydrous sodium sulfate and activated copper  
173 granules in the bottom for dehydration and desulfurization, respectively. 10 g of each  
174 solid sample (soil/sediment) was weighed and wrapped with filter paper, then spiked  
175 with 5.0  $\mu\text{L}$  recovery surrogates ( $200 \text{ mg L}^{-1}$ ) and Soxhlet-extracted for 24 h with 150  
176 mL DCM in a 45 °C water bath. At the same time, activated copper sheets were added  
177 into the flasks for the desulfurization step.

178 The sample (water, sediments and soil) extracts were concentrated to ca. 2-3 mL  
179 and solvent-exchanged to *n*-hexane (GC grade, Tedia, USA) by a rotary evaporator  
180 (Heidolph RE-52, Germany). The concentrated extract was then purified by a column  
181 filled with alumina and silica ( $v/v=1/2$ ), PAH fractions were eluted with a mixed  
182 solution of DCM and *n*-hexane ( $v/v=2/3$ ). The eluent was concentrated to ca. 1 mL by  
183 the same rotary evaporator and transferred to a 2 mL sample vial. The sample volume  
184 was reduced to ca. 0.2 mL with a gentle nitrogen stream (purity > 99.999%). The internal  
185 standards (hexamethylbenzene, purchase from o2si smart solution, USA) were then  
186 spiked into the final samples before GC-MS analysis.

187 A gas chromatography-mass spectrometer (GC-MS, Agilent, 7890N GC-  
188 5975MSD) was used to detect 16 PAHs (Xing et al. 2016): naphthalene (Nap),

189 acenaphthylene (Acy), acenaphthene (Ace), fluorene (Flu), phenanthrene (Phe),  
190 anthracene (Ant), fluoranthene (Fla), pyrene (Pyr), benz(*a*)anthracene (BaA), chrysene  
191 (Chry), benzo(*b*)fluoranthene (BbF), benzo(*k*)fluoranthene (BkF), benzo(*a*)pyrene  
192 (BaP), indeno(1,2,3-*cd*)pyrene (InP), dibenz(*a,h*)anthracene (DahA),  
193 benzo(*ghi*)perylene (BghiP). Further information on PAHs is given in **Table S1**. A fused  
194 quartz capillary chromatographic column (DB-5MS, 30 m×0.25 mm×0.25 μm, Agilent,  
195 USA) was employed to separate the 16 PAHs, and the electron impact ion source was  
196 operated in 70 eV. The temperature program for the chromatographic column was as  
197 follows: kept the initial temperature 80 °C for 2 min, then rose to 290 °C at the rate of  
198 4 °C/min, kept for 25 min. The temperature of the sample inlet was at 280 °C. High-  
199 purity helium (He, 99.999%) was loaded as the carrier gas flowing at 1.0 mL/min. 1.0  
200 μL aliquot of each final sample was injected for analysis at the no-split injection mode.

### 201 **2.3 Quality Assurance /Quality Control (QA/QC)**

202 To ensure the quality of pretreatment and GC-MS analysis, a procedural blank  
203 sample and a parallel sample was set during every batch of the experiments (no more  
204 than 16 samples), a solvent blank sample and a QC standard was injected in each day's  
205 analysis to check the possible interferences and cross-contaminations. No significant  
206 peaks were detected in solvent banks and procedural blanks. The relative deviations of  
207 PAHs in parallel sample analysis were <20%, which is an acceptable error range. The  
208 average recoveries of five deuterated PAH surrogates were in the range of 75.0-120%,  
209 the final results were corrected by recoveries, concentrations for solid samples (soil and  
210 sediments) are expressed in dry weight (dw) basis. For data statistics, concentrations  
211 below the method detection limits (MDLs) were calculated as the half of the MDL  
212 values. The MDLs of PAHs for water and solid samples were in the range of 0.02-1.80  
213 ng L<sup>-1</sup> and 0.01-1.20 ng g<sup>-1</sup> dw, respectively, as listed in **Table S1**.

## 214 3. RESULTS AND DISCUSSION

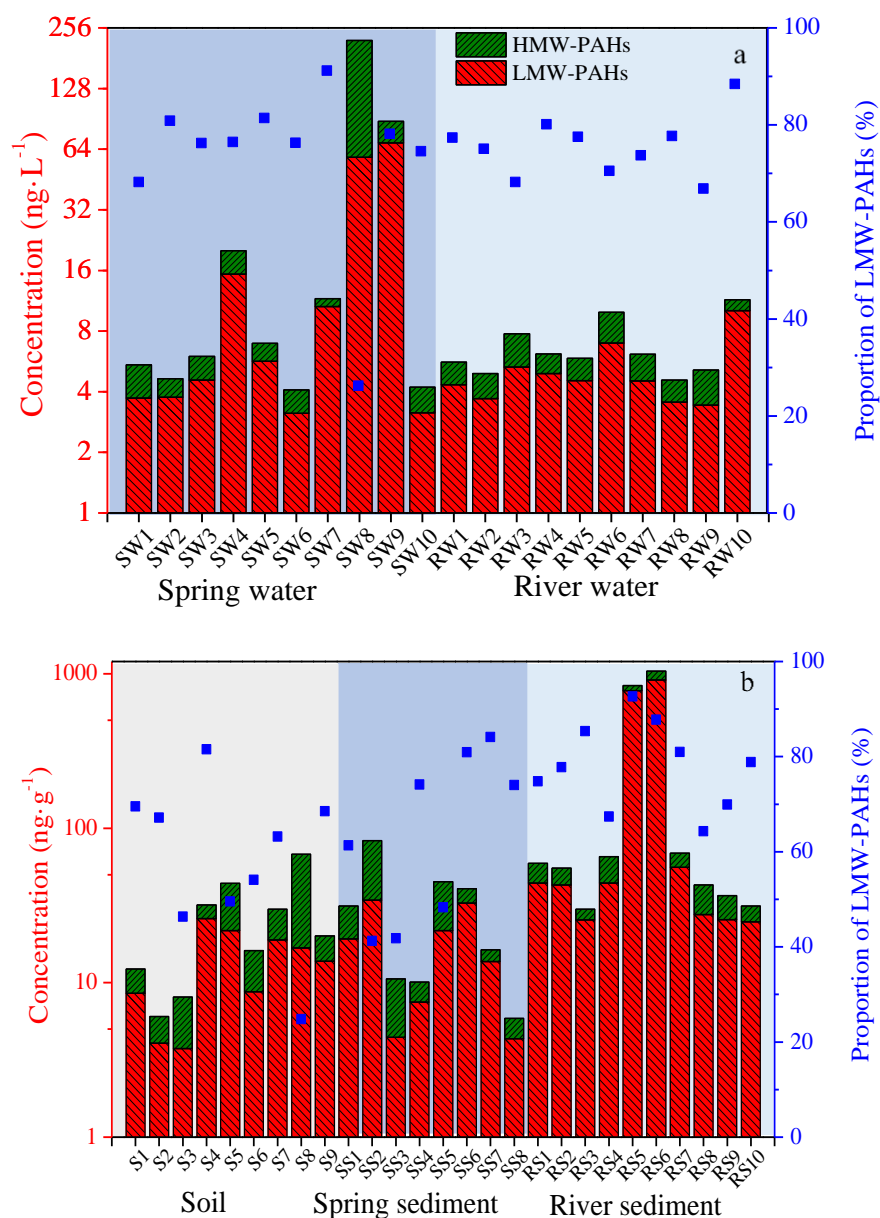
### 215 3.1 Concentrations and distribution of PAHs in multimedia environment

#### 216 3.1.1 PAHs in spring and river water

217 Detection rates of 9 PAHs (Ace, Flu, Ant, Fla, Pyr, BkF, InP, DahA and BghiP)  
218 were < 50% in both river water and spring water. Detection rates for other 5 PAHs (Nap,  
219 Phe, BaA, BbF and BaP) were 100% in the river water, but in spring water only 2 PAHs  
220 (Nap and BbF) were 100% detected (**Table S2**). The more abundant species in river  
221 water than in spring water indicated (1) the possible loss of certain PAHs during the  
222 transport of groundwater (spring water) from the spring outlet to the river water due to  
223 the adsorption by particles and (2) other sources of PAHs in the river water besides the  
224 spring water.

225 The concentrations of  $\Sigma_{16}$ PAHs (sum of total 16 priority PAHs) in the spring  
226 water (range: 4.09-222  $\text{ng}\cdot\text{L}^{-1}$ , average: 37.3  $\text{ng}\cdot\text{L}^{-1}$ ) were higher (not significantly,  $p$   
227 = 0.317, Mann-Whitney test) than those in the river water (range: 4.56-11.4  $\text{ng}\cdot\text{L}^{-1}$ ,  
228 average: 6.75  $\text{ng}\cdot\text{L}^{-1}$ ) (**Figure 2a, Table S2**). This may be attributable to several reasons:  
229 (1) PAHs can quickly enter karst aquifers via the vadose zone because the thin and  
230 uneven soil layer might not be sufficient to filter PAHs from the surface system (**Sun et**  
231 **al. 2019**); (2) abundant precipitation in this area may also enhance the downward  
232 movement of PAHs (**Li et al. 2019**); (3) the highly vulnerable karst area with numerous  
233 sinkholes, fissures and fractures acts as pathways and conduits for rainwater and surface  
234 runoff to enrich pollutants in the spring water (**Qin et al. 2021**). Groundwater can have  
235 the optimum condition for long-term retention of organic pollutants. Because of low  
236 temperature, stable environment, and dormant bacteria with low metabolic activity  
237 (**Ladd et al. 1982**), the degradation of PAHs may be relatively slow. However,  
238 concentrations of  $\Sigma_{16}$ PAHs at SW8 (WZQ, 222  $\text{ng}\cdot\text{L}^{-1}$ ) and SW9 (CSD, 88  $\text{ng}\cdot\text{L}^{-1}$ )  
239 were much higher than those at the other sites (< 20  $\text{ng}\cdot\text{L}^{-1}$ ). Pollution from a pig farm

240 near WZQ and frequent agricultural and human activities near CSD are possible reasons.  
241 Compared to the karst areas in Southwest and North China, the  $\Sigma_{16}$ PAHs  
242 concentrations of groundwater (range: 4.09-222  $\text{ng}\cdot\text{L}^{-1}$ , average: 37.3  $\text{ng}\cdot\text{L}^{-1}$ ) in the  
243 study karst area were lower than those in the underground river from the karst Dashiwei  
244 Tiankeng (range: 54.7-192  $\text{ng}\cdot\text{L}^{-1}$ , average: 102  $\text{ng}\cdot\text{L}^{-1}$ , (Kong et al. 2011)) in Guangxi,  
245 in the Laolongdong karst underground river (range: 289-15200  $\text{ng}\cdot\text{L}^{-1}$ , (Lan et al. 2014))  
246 and epikarst springs (range: 341-4968  $\text{ng}\cdot\text{L}^{-1}$ , (Sun et al. 2014)) from Chongqing, and  
247 in the groundwater (range: 2137-9037  $\text{ng}\cdot\text{L}^{-1}$ , (Shao et al. 2014)) from the Guozhuang  
248 karst system in Shanxi, North of China. Overall, the  $\Sigma_{16}$ PAHs concentrations in the  
249 groundwater from the study area were relatively low across China.



250

251 **Figure 2.** PAHs concentrations (Y-axis in the left is expressed logarithmically) and proportions of  
 252 LMW-PAHs in water (a), and soil and sediment (b); where LMW-PAHs mean low-molecular-weight  
 253 PAHs with 2-3 rings, HMW-PAHs mean high-molecular-weight PAHs with 4-6 rings.

### 254 3.1.2 PAHs in spring and river sediments

255 Concentrations of  $\Sigma_{16}$ PAHs in the spring sediments (range: 5.87-83.0 ng·g<sup>-1</sup>,  
 256 average: 30.3 ng·g<sup>-1</sup>) were significantly lower ( $p=0.017$ , Mann-Whitney test) than  
 257 those in the river sediments (range: 29.9-1041 ng·g<sup>-1</sup>, average: 227 ng·g<sup>-1</sup>) (**Figure 2b**,  
 258 **Table S3**). This is contrary to the result in the water compartment stated above. In  
 259 general, river sediments will reflect the cumulative burden from a wider catchment.

260 Spring sediments received materials from the discharge area (surface runoff and  
261 particles) and underground system (spring water and rock); but the sediments in surface  
262 streams or rivers received materials from the open environment, potentially with  
263 multiple sources of PAHs, such as the inputs from the source water/sediments (spring  
264 water and sediments are essential sources for the surface sediments in the karst area)  
265 and sedimentation from surrounding soils, surface runoff (Sun et al. 2019), and dry and  
266 wet depositions of atmospheric PAHs (Perrette et al. 2013). The matrix compositions  
267 of river sediments is mainly clay minerals, which has high total organic carbon (TOC)  
268 content (Xing et al. 2020) and larger specific surface area, enhancing the sorption  
269 capacity of both LMW-PAHs and HMW-PAHs (Cabrerizo et al. 2011). By contrast,  
270 spring sediments were collected from the outlets of isolated karst springs. The main  
271 matrix component was clastic rocks, which has lower adsorption capacity for PAHs  
272 (especially LMW-PAHs) than clay minerals (Lan et al. 2016). This could also be a  
273 reason why the average proportion of LMW-PAHs (63.2%) in spring sediments was  
274 lower than that of the river sediment (78.5%) (Figure 2b and Figure 3). Additionally,  
275 when the spring water is discharged rapidly at the spring outlet, some LMW-PAHs  
276 might volatilize due to the sudden change in micro-environmental conditions, e.g.,  
277 temperatures, pressures and hydrodynamic conditions (Jiang et al. 2013). The  
278 groundwater temperature is lower than the surface temperature, pressures at the spring  
279 outlet may drop from the karst conduits, and the spring will produce more turbulence  
280 flow once water is released at the surface.

### 281 3.1.3 PAHs in soils

282 Concentrations of  $\Sigma_{16}$ PAHs in soils were in the ranged of 6.04-67.7  $\text{ng}\cdot\text{g}^{-1}$   
283 (average: 25.8  $\text{ng}\cdot\text{g}^{-1}$ ) (Figure 2b, Table S4). Among 16 priority PAHs, 8 compounds  
284 including Nap, Acy, Phe, Pyr, BaA, Chry, BkF and BaP were 100% detected in all the  
285 soil samples of the study area. The detection rate of Ant was only 44.4%, which is  
286 lowest, that may be caused by its rapid photolysis. Nap (average: 4.54  $\text{ng}\cdot\text{g}^{-1}$ ) was the

287 most abundant PAH compound detected in soils, followed by Phe ( $4.03 \text{ ng}\cdot\text{g}^{-1}$ ), Fla  
288 ( $2.73 \text{ ng}\cdot\text{g}^{-1}$ ), Pyr ( $2.54 \text{ ng}\cdot\text{g}^{-1}$ ), BbF ( $2.13 \text{ ng}\cdot\text{g}^{-1}$ ), Chry ( $1.72 \text{ ng}\cdot\text{g}^{-1}$ ), BaA ( $1.53$   
289  $\text{ng}\cdot\text{g}^{-1}$ ), InP ( $1.32 \text{ ng}\cdot\text{g}^{-1}$ ), BaP ( $1.31 \text{ ng}\cdot\text{g}^{-1}$ ) and BghiP ( $1.13 \text{ ng}\cdot\text{g}^{-1}$ ). These listed  
290 PAHs contributed 84.0% of the 16 priority PAHs in the study karst area.

291 Soils from Sites S2 (YQD) and S8 (CSD) had the lowest and highest PAH  
292 concentrations at  $6.04 \text{ ng}\cdot\text{g}^{-1}$  and  $67.7 \text{ ng}\cdot\text{g}^{-1}$ , respectively (**Figure 2b**). The low  
293 concentration of S2 (recharge area of YQD) likely reflects its remote location, which is  
294 distant from any anthropogenic activities. Highly-developed agriculture and dense  
295 population is the likely reason for the high PAH concentrations (S8), since the CSD  
296 karst spring system has a superior hydrogeological condition, which has a relative  
297 water-resisting layer (Shipai Formation ( $\text{C}_{1\text{sh}}$ )) that can retain water to provide suitable  
298 conditions for living and agricultural development.

299 The concentrations of PAHs in the soils (range:  $6.04\text{-}67.7 \text{ ng}\cdot\text{g}^{-1}$ , average:  $25.8$   
300  $\text{ng}\cdot\text{g}^{-1}$ ) from the study karst area were lower than those from other typical karst areas,  
301 such as in the topsoil (range:  $16.9\text{-}190 \text{ ng}\cdot\text{g}^{-1}$ , average:  $58.5 \text{ ng}\cdot\text{g}^{-1}$ , (Wang et al. 2009))  
302 from Guangxi, in karst valley topsoil (range:  $161\text{-}3301 \text{ ng}\cdot\text{g}^{-1}$ , (Zhu et al. 2020)) in  
303 Chongqing, in the soil (average:  $185 \text{ ng}\cdot\text{g}^{-1}$ , (Perrette et al. 2013)) of the mountain  
304 forest karst system from France and in the karst agriculture soil (average:  $3250 \text{ ng}\cdot\text{g}^{-1}$ ,  
305 (Schwarz et al. 2011)) from Germany.

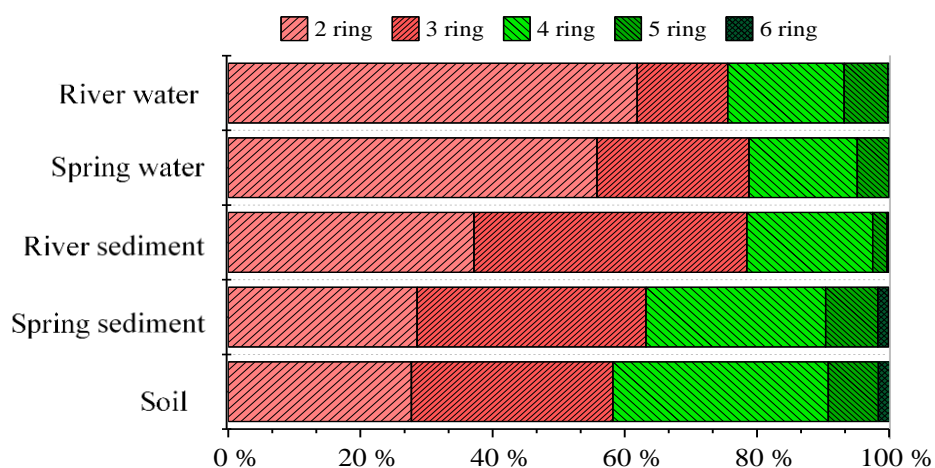
## 306 **3.2 Compositions and possible sources of PAHs**

### 307 **3.2.1 PAHs compositions**

308 Generally, the PAH compositions in this study area varied among different  
309 environmental media (**Figure 3**). The proportions of LMW-PAHs in water, sediments  
310 and soil samples (average 58.2-78.6%) were much higher than those of HMW-PAHs,  
311 which suggested the existence of recent local PAH sources (Shao et al. 2014). The  
312 octanol-water partition coefficients (Kow) (Maliszewska - Kordybach et al. 2007) of

313 PAHs increased with the number of aromatic rings ([Table S1](#)); HMW-PAHs are more  
 314 hydrophobic than LMW-PAHs. Thus, HMW-PAHs are more likely to distribute in the  
 315 particle phases (soil and sediments) rather than in water. Soil layers can filter out PAHs  
 316 by adsorption when PAHs transport to the groundwater ([Sun et al. 2019](#)), which is more  
 317 efficient for HMW compounds ([Lan et al. 2019](#), [Wang et al. 2012](#)). HMW-PAHs  
 318 preferentially tend to bind to particles ([Sun et al. 2009](#), [Wang et al. 2017](#)), and particle-  
 319 promoted transport with rapid water flow may be pivotal for their mobilization to  
 320 sediments and soil ([Schwarz et al. 2011](#)).

321 The average proportion (73.0%) of LMW-PAHs in spring water was similar as that  
 322 in the river water (75.6%) ([Figure 2a](#) and [Figure 3](#)). It indicated the similar PAH  
 323 source in spring water and surface water, e.g., spring water recharged surface water.  
 324 The consistency of the PAH compositions ([Figure 3](#)) in the river water and spring water  
 325 also confirmed the similar sources or/ and transport of PAHs between these two media.  
 326 The PAH compositions in soil were similar to those in spring sediments, showing that  
 327 the soils from recharge areas is the major PAH source in spring sediments.



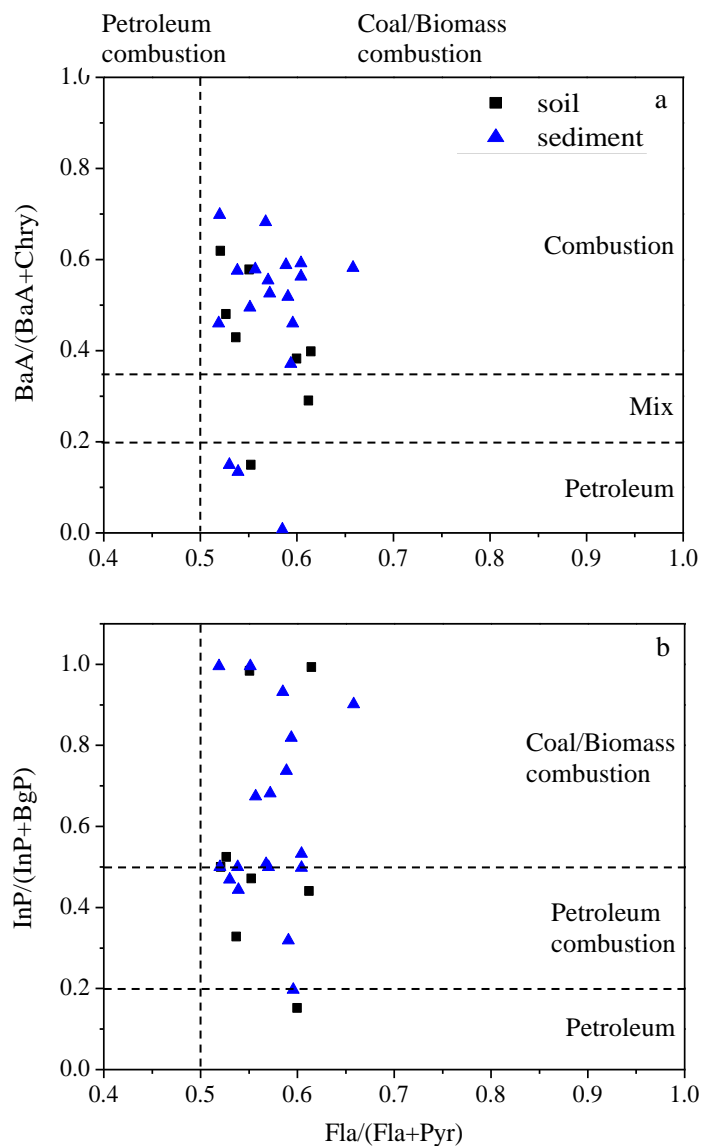
328  
 329 **Figure 3.** Average compositions/ proportions of PAHs in multimedia environment from the karst  
 330 area in Western Hubei, Central China

### 331 3.2.2 PAHs sources

332 The detection rates of some PAHs, especially HMW-PAHs, were quite low in  
 333 water ([Table S2](#), both spring and river water) in this karst area (due to their low

334 concentrations and poor water solubility). Soil is the primary sink of contaminants in  
335 the karst systems (Qu et al. 2019), sediments come from soil transport and  
336 sedimentation. PAHs are more stable in the solid phases than liquid phases, so the  
337 measurements of soil and sediments (spring sediments and river sediments) were used  
338 to diagnose the PAHs sources in this area.

339 The characteristic ratios method has been widely applied to identify the PAH  
340 sources (Guo et al. 2009, Lan et al. 2016, Santino 2010, Sun et al. 2017, Yunker et al.  
341 2002). According to Yunker et al. (2002), the following ratios can be used to identify  
342 the PAH sources: 1) the ratio of Fla/(Fla + Pyr) < 0.40, between 0.40-0.50, and > 0.50  
343 indicates petroleum source, petroleum combustion, and biomass and coal combustion,  
344 respectively; 2) the ratio of BaA/(BaA + Chry) < 0.20, between 0.20-0.35, and > 0.35  
345 means petroleum source, petroleum or mixed source of combustion, and combustion  
346 source; 3) the ratio of InP/(InP + BghiP) < 0.20, between 0.20 and 0.50, and > 0.50  
347 indicates petroleum source, petroleum combustion, and biomass or coal burning.



348

349 **Figure 4.** Plots for the characteristic ratios of BaA/(BaA+Chry) vs. Fla/(Fla+Pyr) (a), and  
 350 InP/(InP+BghiP) vs. Fla/(Fla+Pyr) (b) for PAHs

351 The diagnostic ratios of Fla/(Fla+Pyr) were in the range of 0.52-0.66 (**Figure 4**)  
 352 indicating major source of the incomplete combustion of coal and biomass (such as  
 353 grass, wood, etc.). **Figure 4a** showed that the ratios of BaA/(BaA+Chry) for most sites  
 354 were > 0.35 and only 5 of them were < 0.20, suggesting that PAHs have mixed  
 355 combustion and petrogenic sources, in which most PAHs were derived from high-  
 356 temperature combustion. Similarly, the InP/(InP+BghiP) ratios are mostly > 0.20 in the  
 357 karst area, suggesting coal/biomass and petroleum incomplete combustion are the main

358 sources. Overall, the characteristic ratios method shows that the mixed sources from  
359 high-temperature combustion of petroleum, biomass and coal, were the major PAH  
360 sources in this karst area of Western Hubei, in which coal and biomass combustion were  
361 dominant. This result was in accordance with the actual socioeconomic circumstances  
362 in the study area: besides coal, biomass such as the wood and straw could be still an  
363 important energy source in the undeveloped area.

364 Principal component analysis (PCA) method was applied to identify possible  
365 contributions from different sources of PAHs. The rotated factors of 16 priority PAHs  
366 from the study area are listed in [Table S5](#). The analysis shows that four principal  
367 components explained approximately 38.4%, 32.6%, 28.1% and 0.9% of the total  
368 variance, respectively, and the top three principal components accounted for 99.1% in  
369 total contribution.

370 Factor 1 was dominated by Acy, Chry, BbF, BkF, BaP, InP, DahA and BghiP.  
371 Among these compounds, BbF and BkF are the typical indicator compounds for coal  
372 combustion ([Bao et al. 2020](#)), considerable Chry and BaP were also produced by coal  
373 combustion ([Chen et al. 2005](#), [Li et al. 2003](#)). HMW-PAHs, including InP, DahA and  
374 BghiP, are normally from the processes of high-temperature combustion ([Mai et al.  
375 2003](#)), such as gasoline and diesel combustion and emission ([Simcik et al. 1999](#)).  
376 Therefore, Factor 1 was suggested as coal combustion and vehicle emission sources,  
377 contributing 38.4% of the total PAH sources. Factor 2 was highly weighted by Nap, Flu,  
378 Phe and Ant. Flu and Ant are considered to be the tracer compounds of biomass  
379 combustion, such as wood/grass burning ([Zhang et al. 2020](#)). Thus, Factor 2 can  
380 represent the biomass combustion source and explained 32.6% of the total PAH sources.  
381 Factor 3 was mainly composed of Fla, Pyr and BaA. Fla and Pyr are indicator  
382 compounds for coal combustion ([Bao et al. 2020](#), [Simcik et al. 1999](#)). Thus, Factor 3  
383 was identified as coal combustion source, and it was responsible for 28.1% of the total  
384 PAH sources. Factor 4 was dominated by Ace, which is the dominant molecular  
385 signature compound in the petrogenic sources, but it is only 0.9%, we can neglect it.

386 The PCA results were consistent with those from characteristic ratios for source  
387 apportionment, indicating that the PAH sources were well diagnosed in our study.

388 Vehicle emissions have increased in this study area due to the development of  
389 tourism and the improvement of people living standards recently (Zhao et al. 2021).  
390 Coal is the most important energy in China, and the proportion of coal consumption has  
391 decreased by years, it accounted for 57.7% of the total energy consumption in 2019  
392 (National Bureau of Statistics of China 2020). According to the statistical data for the  
393 rural renewable fuel and satellite remoting sensing, 48% of straw were treated by  
394 burning in Hubei province, and the total emission of PAHs from straw combustion  
395 decreased due to the prohibition on open burning of straw (Satellite Environmental  
396 Centre 2016). Coal combustion, biomass burning and vehicle emission are the major  
397 PAH sources in China (Han et al. 2019). In our study, they account for about 99.1% of  
398 PAH sources in the karst area of the western Hubei, Central China. Thus, the PAH  
399 source diagnosis in this study area was consistent with the energy consumption in China.

### 400 **3.3 PAHs transport in karst spring systems**

#### 401 **3.3.1 Transport regularity of PAHs in karst spring systems**

402 According to the study by Medici et al. (2019), contaminants from the recharge  
403 area can reach the groundwater via the fractures and conduits in karst area, and then are  
404 discharged rapidly in spring outlets; at the same time, some particles and silt were  
405 washed out and then deposited by the spring outlet. The change of PAH compositions  
406 in the multimedia environment during their transport in the 10 karst spring systems is  
407 shown in Figure S1. Overall, the compositions of PAHs were similar among the soil,  
408 spring sediments and spring water in the same karst spring systems. Spearman  
409 correlation coefficients ( $\rho$ ) were calculated for PAH compositions between paired  
410 samples (recharge area soil and spring sediments, spring water and spring sediments,  
411 and spring water and discharge area soil), to observe the correlations of PAH

412 compositions in 10 karst spring systems (**Table 1**). Significant correlations of PAH  
 413 compositions were found in most of the karst spring systems, especially in the YQD,  
 414 XYD, and FD karst spring systems: the correlation coefficients reached 0.86 and 0.92  
 415 between recharge area soil and spring sediments, and between spring water and spring  
 416 sediments in the YQD spring system, respectively; the correlation coefficients of PAH  
 417 compositions reached 0.59 and 0.78 between spring water and spring sediments, and  
 418 between spring water and discharge area soil respectively, in the XYD spring system.  
 419 It indicated that the PAHs transmitted from the recharge area soil to spring sediments  
 420 and the discharge area soil, i.e., the recharge area was the source of PAHs for discharge  
 421 area. However, there is a poor correlation ( $\rho = 0.07$ ) between the recharge area soil and  
 422 spring sediments in the CSD spring system. This may reflect the different pollution  
 423 sources and different transport paths (Sun et al. 2019, Yuan 2000), which will be  
 424 discussed in Section 3.3.2.

425 **Table 1.** Spearman correlation coefficients ( $\rho$ ) of PAH compositions in different environment media  
 426 at the karst spring systems

Spring Correlation	MGQ	YQD	JZZQ	CSD	ZPLD	DYQ	XYD	FD	XCC
Recharge area soil- spring sediment	0.55*	0.86**	0.88**	0.07	-	-	-	-	-
Spring water-spring sediment	0.57*	0.92**	0.31	0.70**	0.31	0.41	0.59*	0.51*	-
Spring water- discharge area soil	-	0.58*	-	-	-	-	0.78**	0.51*	0.66**

427 \*: Correlation is significant at 0.05 level (2-tailed); \*\*: Correlation is significant at 0.01 level (2-  
 428 tailed); -: lack of data for calculation.

### 429 3.3.2 PAHs transport characteristics in typical karst spring systems

430 Hydrogeological conditions (e.g., stratum and geological structure) and their  
 431 hydrodynamic characteristics will affect PAH transport, so it is necessary to study PAH  
 432 transport with different hydrogeological conditions. Soil, surface water and surface  
 433 sediments in a karst system can be transported to the underground river by fast-flowing

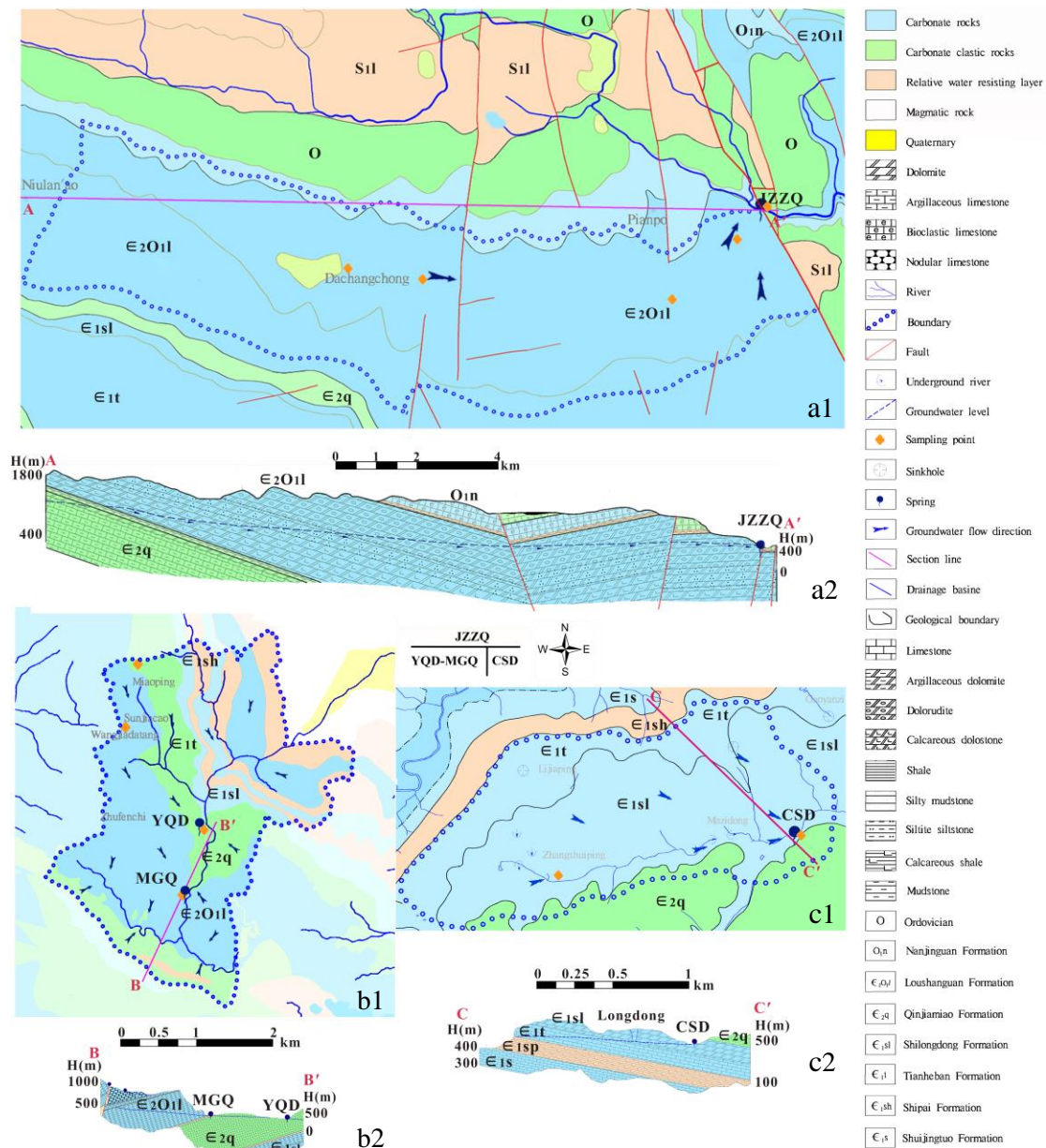
434 conduit water or slow-flowing fissure water (Lan et al. 2018). Still, there are some  
435 differences among different karst spring systems. According to the actual  
436 hydrogeological conditions (Figure 5), three (or four) karst spring systems (JZZQ,  
437 MGQ-YQD and CSD) were taken for examples to analyze the transport characteristics  
438 in different hydrogeological conditions.

439 The JZZQ spring system is located in the dolerudite rocks of the Loushanguan  
440 Formation ( $C_2O_{11}$ ) with some faults developed near the spring (Figure 5 a1 and a2).  
441 Normally, bedding plane fractures of dolostone aquifer dominate the groundwater flow  
442 at shallow depths. They are sub-horizontal, sub-parallel and laterally persistent (Medici  
443 et al. 2019). While the faults developed proximity to the spring can provide the  
444 longitudinal channels for the groundwater flow. Both longitudinal and bedding-plane  
445 directions flows of groundwater would raise turbulent flows. The particles and  
446 sediments in karst conduits were easily washed out by turbulence. They then deposited  
447 at the spring outlet, causing the increased PAHs content in spring sediments. The  
448 multiple linear regression analysis (MLRA) (Larsen and Baker 2003) was applied to  
449 quantitatively evaluate the PAH transport in these karst spring systems. The compositions  
450 of PAHs in the recharge-area soil and spring water, and in the spring sediments were  
451 used as two independent variables and the dependent variable, respectively, when  
452 running the MLRA. The MLRA results partly confirmed this process, which indicated  
453 that the recharge area soil made significant ( $p=0.013$ ) contribution of PAHs to spring  
454 sediments, and the transport from the soils in recharge areas explained 51.4% of PAHs  
455 in spring sediments.

456 The YQD-MGQ spring system is located in dolomite rocks of the Loushanguan  
457 Formation ( $C_2O_{11}$ ), a strong permeable stratum convenient for particulates and  
458 sediments flowing along the underground river (Figure 5 b1 and b2). The lithology of  
459 YQD is carbonate clastic rocks (also argillaceous limestone rocks) of the Qinjiamiao  
460 Formation ( $C_2q$ ), which is a weak permeable aquifer (Figure 5 b1 and b2). The  
461 concentration of HMW-PAHs in the spring sediments in MGQ was higher than that in

462 YQD (**Figure 2b**). It indicated that the strong permeable stratum is conducive to the  
463 rapid transport of organic pollutants, and the particulate matter may be the leading  
464 carriers of HMW-PAHs (**Levy et al. 2017**). While in the weak permeable aquifer,  
465 HMW-PAHs are easily hindered and adsorbed by carbonate rock debris and deposited  
466 in karst conduit (**Ma et al. 2017**). The MLRA results showed that the transport of PAHs  
467 from both the soil and spring water could explain 20.6% and 96.2% ( $R^2=0.206, 0.962$ )  
468 of the PAHs in the spring sediments of MGQ and YQD spring systems, respectively.  
469 For the YQD spring system, both the recharge area soil ( $p=0.026$ ) and the spring water  
470 ( $p<0.001$ ) made significant PAH contributions to the spring sediments: transport from  
471 the recharge-area soil and spring water explained 28.6% and 67.6% of PAHs in the  
472 spring sediments, respectively.

473 CSD karst spring is a siphonal spring (**Guo et al. 2020**), it had two groundwater  
474 flow systems: the dolomite of Shilongdong Formation ( $C_{1sl}$ ) groundwater system and  
475 the limestone of Tianheban Formation ( $C_{1t}$ ) groundwater system (**Figure 5 c1 and c2**).  
476 The underneath is a calcareous shale of Shipai Formation ( $C_{1sh}$ ), a low-permeability  
477 layer that can prevent groundwater loss. The development of the karst conduits  
478 penetrated in these two groundwater systems, and siphon structure was developed in  
479 the limestone aquifer ( $C_{1t}$ ) and connected with the solution cavity, thus forming the  
480 characteristics of intermittent discharge from CSD karst spring during the no-rain  
481 period. The PAHs concentration in spring sediments was relatively low though it is the  
482 most polluted area in the study area. It is speculated that the collected soil sample cannot  
483 represent the whole recharge area of CSD (can be seen from **Figure 5 c1**), but the  
484 sources of sediments are from the whole recharge area. There are still some other  
485 slightly-polluted recharge areas (in the north part) that were not sampled in this study.  
486 The diverse sources of spring sediments caused the diverse PAH sources in the  
487 sediments, leading to the low concentrations of PAHs and insignificant correlation  
488 between the spring sediments and soil in the CSD system.



489  
 490 **Figure 5.** The hydrogeological profiles of JZZQ (a1 and a2), YQD-MGQ (b1 and b2) and CSD (c1  
 491 and c2) karst spring systems

492 **4. CONCLUSIONS**

493 The PAH concentrations were relatively low in surface soil and groundwater/spring  
 494 water from the typical karst area of Central China. The  $\sum_{16}$ PAHs in the surface water  
 495 were lower than those in the spring water. However, the pattern in sediments was  
 496 contrary: the concentrations of  $\sum_{16}$ PAHs in the surface/river sediments were

497 significantly higher than those in the spring sediments. This could be due to different  
498 sources of PAHs and different matrix compositions in the sediments: the surface  
499 sediments from the open environment had multiple sources of PAHs, and their matrix  
500 component is mainly clay minerals with strong sorption capacity of PAHs. While the  
501 source of spring sediments was solely from the isolated environment, and their main  
502 matrix component is clastic rocks with relatively weaker adsorption on LMW-PAHs  
503 than clay minerals. Besides, the average proportion of LMW-PAHs in the surface  
504 sediments was higher than that in the spring sediments. LMW-PAHs were predominated  
505 in the soil, water and sediments, and the proportion of LMW-PAHs in sediments was  
506 higher than that in soil. Biomass burning, coal combustion and vehicle emission are the  
507 major sources of PAHs.

508 Our results highlighted the process and characteristics of PAH transport in the karst  
509 spring systems: Significant correlations of PAH compositions in the different karst  
510 spring systems were observed. Due to the high dynamic of karst spring systems and the  
511 rapid transport of PAHs in various media without significant degradation, the  
512 vulnerability of groundwater in karst area is revealed. We can conclude that  
513 hydrogeological conditions will affect PAH transport: the strong permeable stratum is  
514 conducive to the rapid transport of particles, leading to a higher proportion of HMW-  
515 PAHs in the sediment at the spring outlet.

## 516 CREDIT AUTHORSHIP CONTRIBUTION STATEMENT

517 **Wei Chen:** Investigation, Methodology, Resources, Writing - original draft,  
518 Writing - review & editing. **Ziqiong Zhang:** Formal analysis, Data curation,  
519 Visualization, Writing - original draft. **Ying Zhu:** Methodology, Formal analysis,  
520 Writing - review & editing. **Zhenxian Wang:** Formal analysis, Writing - review &  
521 editing. **Longliang Wang:** Investigation, Methodology, Writing - review & editing.  
522 **Junwu Xiong:** Formal analysis, Writing - review & editing. **Zhe Qian:** Formal analysis,  
523 Methodology, Writing - review & editing. **Shuai Xiong:** Visualization, Writing - review

524 & editing. **Ruichao Zhao**: Visualization, Writing - review & editing. **Wei Liu**:  
525 Investigation, Conceptualization, Methodology, Resources, Writing - review & editing,  
526 Supervision. **Qiuke Su**: Data curation, Methodology, Writing - review & editing.  
527 **Jiangang Zhou**: Data curation, Writing - review & editing. **Hou Zhou**: Supervision,  
528 Funding acquisition. **Shihua Qi**: Resources, Supervision. **Kevin C. Jones**: Supervision,  
529 Methodology, Writing - review & editing.

## 530 **DECLARATION OF COMPETING INTEREST**

531 The authors declare that they have no known competing financial interests or  
532 personal relationships that could have appeared to influence the work reported in this  
533 paper.

## 534 **ACKNOWLEDGEMENTS**

535 This study was jointly funded by National Key Research and Development  
536 Program (2019YFC1805502), National Natural Science Foundation of China  
537 (41907327 and 42007178), Guangxi Key Science and Technology Innovation Base on  
538 Karst Dynamics (KDL & Guangxi202002), Natural Science Foundation of Hubei  
539 (2019CFB372 and 2020CFB463), Open Funds from State Key Laboratory of Organic  
540 Geochemistry (SKLOG202008), China Geological Survey (DD20190824),  
541 Fundamental Research Funds for the Central Universities (CUG 190644 and  
542 CUGL180817), and Open Funds from Hubei Key Laboratory of Environmental Water  
543 Science in the Yangtze River Basin, and Open Funds Institute of Quality Standard and  
544 Testing Technology, Beijing Academy of Agriculture and Forestry Sciences  
545 (ZBZX202106). The authors would like to express their grateful thanks to Po Peng for  
546 field sampling, to Zhaoyang Wei and Chang Pu for sample pretreatment, to the  
547 anonymous reviewers for comments and suggestions in improving the manuscript and  
548 special thanks to Julia Ellis Burnet for always help of English proofing.

549 **REFERENCES**

- 550 Bao, K., Zaccone, C., Tao, Y., Wang, J., Shen, J. and Zhang, Y. (2020) Source  
551 apportionment of priority PAHs in 11 lake sediment cores from Songnen Plain,  
552 Northeast China. *Water Research* 168(1), 115158.
- 553 Cabrerizo, A., Dachs, J., Moeckel, C., Ojeda, M.-J., Caballero, G., Barceló, D. and  
554 Jones, K.C. (2011) Ubiquitous net volatilization of polycyclic aromatic hydrocarbons  
555 from soils and parameters influencing their soil-air partitioning. *Environmental Science  
556 & Technology* 45(11), 4740-4747.
- 557 Chen, Y., Sheng, G., Bi, X., Feng, Y., Mai, B. and Fu, J. (2005) Emission factors for  
558 carbonaceous particles and polycyclic aromatic hydrocarbons from residential coal  
559 combustion in China. *Environmental Science & Technology* 39(6), 1861-1867.
- 560 Guo, W., He, M., Yang, Z., Lin, C., Quan, X. and Men, B. (2009) Distribution,  
561 partitioning and sources of polycyclic aromatic hydrocarbons in Daliao River water  
562 system in dry season, China. *Journal of Hazardous Materials* 164(2-3), 1379-1385.
- 563 Guo, X., Chen, Q., Huang, K. and Zhou, H. (2020) Dynamic features and causes of  
564 Chaoshuidong Siphonal Spring. *Earth Science (in Chinese with English abstract)*  
565 45(12), 4524-4534.
- 566 Han, J., Liang, Y., Zhao, B., Wang, Y., Xing, F. and Qin, L. (2019) Polycyclic aromatic  
567 hydrocarbon (PAHs) geographical distribution in China and their source, risk  
568 assessment analysis. *Environmental Pollution* 251, 312-327.
- 569 Huang, H., Liu, H., Xiong, S., Zeng, F., Bu, J., Zhang, B., Liu, W., Zhou, H., Qi, S., Xu,  
570 L. and Chen, W. (2021) Rapid transport of organochlorine pesticides (OCPs) in  
571 multimedia environment from karst area. *Science of the Total Environment* 775,  
572 145698.
- 573 Jiang, Y., Hu, Y. and Schirmer, M. (2013) Biogeochemical controls on daily cycling of  
574 hydrochemistry and  $\delta^{13}C$  of dissolved inorganic carbon in a karst spring-fed pool.  
575 *Journal of Hydrology* 478(25), 157-168.
- 576 Kong, X., Qi, S., Oramah, I.T., Zhang, Y. and He, S.-Y. (2011) Contamination of  
577 polycyclic aromatic hydrocarbons in surface water in underground river of Dashiwei  
578 Tiangkeng group in karst area, Guangxi. *Environmental Science (in Chinese with  
579 English abstract)* 32(4), 1081-1087.
- 580 Ladd, T.I., Ventullo, R.M., Wallis, P.M. and Costerton, J.W. (1982) Heterotrophic  
581 activity and biodegradation of labile and refractory compounds by groundwater and  
582 stream microbial populations. *Applied and Environmental Microbiology* 44(2), 321-  
583 329.
- 584 Lan, J., Sun, Y., Tian, P., Lu, B., Shi, Y., Xu, X., Liang, Z. and Yang, P. (2014)  
585 Contamination and ecological risk assessment of polycyclic aromatic hydrocarbons in  
586 water and in Karst underground river catchment. *Environmental Science (in Chinese  
587 with English abstract)* 35(10), 3722-3730.
- 588 Lan, J., Sun, Y. and Xiang, X. (2019) Ecological risk assessment of PAHs in a karst  
589 underground river system. *Polish Journal of Environmental Studies* 29(1), 677-687.

590 Lan, J., Sun, Y., Xiao, S. and Yuan, D. (2016) Polycyclic aromatic hydrocarbon  
591 contamination in a highly vulnerable underground river system in Chongqing,  
592 Southwest China. *Journal of Geochemical Exploration* 168, 65-71.

593 Lan, J., Sun, Y. and Yuan, D. (2018) Transport of polycyclic aromatic hydrocarbons in  
594 a highly vulnerable karst underground river system of southwest China. *Environmental*  
595 *Science and Pollution Research* 25(34), 34519-34530.

596 Larsen, R.K. and Baker, J.E. (2003) Source apportionment of polycyclic aromatic  
597 hydrocarbons in the urban atmosphere: a comparison of three methods. *Environmental*  
598 *Science & Technology* 37(9), 1873-1881.

599 Levy, W., Pandelova, M., Henkelmann, B., Bernhöft, S., Fischer, N., Antritter, F. and  
600 Schramm, K.W. (2017) Persistent organic pollutants in shallow percolated water of the  
601 Alps karst system (Zugspitze summit, Germany). *Science of the Total Environment*  
602 579(1), 1269-1281.

603 Li, A., Jang, J.K. and Scheff, P.A. (2003) Application of EPA CMB8.2 model for source  
604 apportionment of sediment PAHs in Lake Calumet, Chicago. *Environmental Science &*  
605 *Technology* 37(13), 2958-2965.

606 Li, C., Zhang, X., Gao, X., Qi, S. and Wang, Y. (2019) The potential environmental  
607 impact of PAHs on soil and water resources in air deposited coal refuse sites in  
608 Niangziguan karst catchment, Northern China. *International Journal of Environmental*  
609 *Research and Public Health* 16(8), 16081368.

610 Ligaray, M., Baek, S.S., Kwon, H.O., Choi, S.D. and Cho, K.H. (2016) Watershed-scale  
611 modeling on the fate and transport of polycyclic aromatic hydrocarbons (PAHs).  
612 *Journal of Hazardous Materials* 320(15), 23-30.

613 Liu, W., Wang, Z., Chen, Q., Yan, Z., Zhang, T., Han, Z., Chen, W. and Zhou, H. (2020)  
614 An interpretation of water recharge in karst trough zone as determined by high-  
615 resolution tracer experiments in western Hubei, China. *Environmental Earth Sciences*  
616 79(14), 1-13.

617 Ma, J., Liu, H., Tong, L., Wang, Y., Liu, S., Zhao, L. and Hou, L. (2017) Source  
618 apportionment of polycyclic aromatic hydrocarbons and n-alkanes in the soil-sediment  
619 profile of Jiangnan Oil Field, China. *Environmental Science and Pollution Research*  
620 24(15), 13344-13351.

621 Mai, B., Qi, S., Zeng, E.Y., Yang, Q., Zhang, G., Fu, J., Sheng, G., Peng, P. and Wang,  
622 Z. (2003) Distribution of polycyclic aromatic hydrocarbons in the coastal region off  
623 Macao, China: assessment of input sources and transport pathways using compositional  
624 analysis. *Environmental Science & Technology* 37(21), 4855-4863.

625 Maioli, O.L.G., Rodrigues, K.C., Knoppers, B.A. and Azevedo, D.A. (2011)  
626 Distribution and sources of aliphatic and polycyclic aromatic hydrocarbons in  
627 suspended particulate matter in water from two Brazilian estuarine systems.  
628 *Continental Shelf Research* 31(10), 1116-1127.

629 Maliszewska - Kordybach, B., Klimkowicz - Pawlas, A., Smreczak, B. and  
630 Janusauskaite, D. (2007) Ecotoxic effect of phenanthrene on nitrifying bacteria in soils  
631 of different properties. *Journal of Environmental Quality* 36(6), 1635-1645.

632 Medici, G., West, L.J. and Banwart, S.A. (2019) Groundwater flow velocities in a  
633 fractured carbonate aquifer-type: Implications for contaminant transport. *Journal of*  
634 *Contaminant Hydrology* 222, 1-16.

635 Moeckel, C., Monteith, D.T., Llewellyn, N.R., Henrys, P.A. and Pereira, M.G. (2014)  
636 Relationship between the concentrations of dissolved organic matter and polycyclic  
637 aromatic hydrocarbons in a typical U.K. upland stream. *Environmental Science &*  
638 *Technology* 48(1), 130-138.

639 National Bureau of Statistics of China (2020) China energy statistical yearbook China  
640 statistics press, Beijing, <http://www.stats.gov.cn/tjsj/ndsj/2020/indexch.htm>.

641 Niu, S., Dong, L., Zhang, L., Zhu, C., Hai, R. and Huang, Y. (2017) Temporal and  
642 spatial distribution, sources, and potential health risks of ambient polycyclic aromatic  
643 hydrocarbons in the Yangtze River Delta (YRD) of eastern China. *Chemosphere* 172,  
644 72-79.

645 Perrette, Y., Poulenard, J., Durand, A., Quiers, M., Malet, E., Fanget, B. and  
646 Naffrechoux, E. (2013) Atmospheric sources and soil filtering of PAH content in karst  
647 seepage waters. *Organic Geochemistry* 65, 37-45.

648 Qian, Z., Mao, Y., Xiong, S., Peng, B., Liu, W., Liu, H., Zhang, Y., Chen, W., Zhou, H.  
649 and Qi, S. (2020) Historical residues of organochlorine pesticides (OCPs) and  
650 polycyclic aromatic hydrocarbons (PAHs) in a flood sediment profile from the  
651 Longwang Cave in Yichang, China. *Ecotoxicology and Environmental Safety* 196,  
652 110542.

653 Qin, W., Han, D., Song, X. and Liu, S. (2021) Environmental isotopes ( $\delta^{18}\text{O}$ ,  $\delta^2\text{H}$ ,  
654  $^{222}\text{Rn}$ ) and hydrochemical evidence for understanding rainfall-surface water-  
655 groundwater transformations in a polluted karst area. *Journal of Hydrology* 592,  
656 125748.

657 Qu, C., Albanese, S., Lima, A., Hope, D., Pond, P., Fortelli, A., Romano, N., Cerino, P.,  
658 Pizzolante, A. and De Vivo, B. (2019) The occurrence of OCPs, PCBs, and PAHs in the  
659 soil, air, and bulk deposition of the Naples metropolitan area, southern Italy:  
660 Implications for sources and environmental processes. *Environment International* 124,  
661 89-97.

662 Santino, O. (2010) Assessment of polycyclic aromatic hydrocarbons (PAHs) in soil of  
663 a Natural Reserve (Isola delle Femmine) (Italy) located in front of a plant for the  
664 production of cement. *Journal of Hazardous Materials* 173(1-3), 358-368.

665 Satellite Environmental Centre (2016) Satellite-remote-sensing-based monitoring of  
666 straw burning, <http://datacenter.mep.gov.cn>.

667 Schwarz, K., Gocht, T. and Grathwohl, P. (2011) Transport of polycyclic aromatic  
668 hydrocarbons in highly vulnerable karst systems. *Environmental Pollution* 159(1), 133-  
669 139.

670 Shao, Y., Wang, Y., Xu, X., Wu, X., Jiang, Z., He, S. and Qian, K. (2014) Occurrence  
671 and source apportionment of PAHs in highly vulnerable karst system. *Science of the*  
672 *Total Environment* 490(15), 153-160.

673 Simcik, M.F., Eisenreich, S.J. and Liroy, P.J. (1999) Source apportionment and

674 source/sink relationships of PAHs in the coastal atmosphere of Chicago and Lake  
675 Michigan. *Atmospheric Environment* 33(30), 5071-5079.

676 Simmleit, N. and Herrmann, R. (1987) The behavior of hydrophobic, organic  
677 micropollutants in different Karst water systems. *Water, Air, and Soil Pollution* 34(1),  
678 97-109.

679 Sun, J., Wang, G., Chai, Y., Zhang, G., Li, J. and Feng, J. (2009) Distribution of  
680 polycyclic aromatic hydrocarbons (PAHs) in Henan Reach of the Yellow River, Middle  
681 China. *Ecotoxicology and Environmental Safety* 72(5), 1614-1624.

682 Sun, Y., Shen, L. and Yuan, D. (2014) Contamination and source of polycyclic aromatic  
683 hydrocarbons in epikarst spring water. *Environmental Science (in Chinese with English*  
684 *abstract)* 35(6), 2091-2098.

685 Sun, Y., Zhang, S., Lan, J., Xie, Z., Pu, J., Yuan, D., Yang, H. and Xing, B. (2019)  
686 Vertical migration from surface soils to groundwater and source appointment of  
687 polycyclic aromatic hydrocarbons in epikarst spring systems, southwest China.  
688 *Chemosphere* 230, 616-627.

689 Sun, Y., Zhang, S., Xie, Z., Lan, J., Li, T., Yuan, D., Yang, H. and Xing, B. (2020)  
690 Characteristics and ecological risk assessment of polycyclic aromatic hydrocarbons in  
691 soil seepage water in karst terrains, southwest China. *Ecotoxicology and Environmental*  
692 *Safety* 190(1), 110122.

693 Sun, Z., Zhu, Y., Zhuo, S., Liu, W., Zeng, E.Y., Wang, X., Xing, B. and Tao, S. (2017)  
694 Occurrence of nitro- and oxy-PAHs in agricultural soils in eastern China and excess  
695 lifetime cancer risks from human exposure through soil ingestion. *Environment*  
696 *International* 108, 261-270.

697 Wang, C., Wu, S., Zhou, S., Shi, Y. and Song, J. (2017) Characteristics and source  
698 identification of polycyclic aromatic hydrocarbons(PAHs) in urban soils: A review.  
699 *Pedosphere* 27(1), 17-26.

700 Wang, Y., Qi, S., Chen, J., Oramah, T.I. and Yuan, D. (2009) Concentration, distribution  
701 and sources of polyaromatic hydrocarbons in soils from the Karst tiankengs, South  
702 China. *Bulletin of Environmental Contamination and Toxicology* 83(5), 720-726.

703 Wang, Y., Xue, R., Li, J., Zhu, H., Xu, Y., Xue, B., Qi, S., Yuan, D. and Theodore, O.I.  
704 (2012) Compositional fractionation of polyaromatic hydrocarbons in the karst soils,  
705 South China. *Environmental Earth Sciences* 66(7), 2013-2019.

706 Xing, X., Mao, Y., Hu, T., Tian, Q., Chen, Z., Liao, T., Zhang, Z., Zhang, J., Gu, Y.,  
707 Bhutto, S.u.a. and Qi, S. (2020) Spatial distribution, possible sources and health risks  
708 of PAHs and OCPs in surface soils from Dajiuhu Sub-alpine Wetland, central China.  
709 *Journal of Geochemical Exploration* 208, 106393.

710 Xing, X., Zhang, Y., Yang, D., Zhang, J., Chen, W., Wu, C., Liu, H. and Qi, S. (2016)  
711 Spatio-temporal variations and influencing factors of polycyclic aromatic hydrocarbons  
712 in atmospheric bulk deposition along a plain-mountain transect in western China.  
713 *Atmospheric Environment* 139, 131-138.

714 Yuan, D. (2000) Some opinions on geological survey of groundwater resources and  
715 ecological environment in karst mountain area of South China. *Carsologica Sinica (in*

716 Chinese with English abstract) 19(2), 2-7.  
717 Yunker, M.B., Macdonald, R.W., Vingarzan, R., Mitchell, R.H., Goyette, D. and  
718 Sylvestre, S. (2002) PAHs in the Fraser River basin: a critical appraisal of PAH ratios  
719 as indicators of PAH source and composition. *Organic Geochemistry* 33(4), 489-515.  
720 Zeng, F., Jiang, Z., Shen, L., Chen, W., Yang, Q. and Zhang, C. (2018) Assessment of  
721 multiple and interacting modes of soil loss in the karst critical zone, Southwest China  
722 (SWC). *Geomorphology* 322(1), 97-106.  
723 Zhang, R., Li, T., Russell, J., Zhang, F., Xiao, X., Cheng, Y., Liu, Z., Guan, M. and Han,  
724 Q. (2020) Source apportionment of polycyclic aromatic hydrocarbons in continental  
725 shelf of the East China Sea with dual compound-specific isotopes ( $\delta^{13}\text{C}$  and  $\delta^2\text{H}$ ).  
726 *Science of the Total Environment* 704(20), 135459.  
727 Zhang, Z., Chen, X. and Soulsby, C. (2017) Catchment - scale conceptual modelling of  
728 water and solute transport in the dual flow system of the karst critical zone.  
729 *Hydrological Processes* 31(19), 3421-3436.  
730 Zhao, Z., Gong, X., Zhang, L., Jin, M., Cai, Y. and Wang, X. (2021) Riverine transport  
731 and water-sediment exchange of polycyclic aromatic hydrocarbons (PAHs) along the  
732 middle-lower Yangtze River, China. *Journal of Hazardous Materials* 403(5), 123973.  
733 Zhu, L., Lan, J., Sun, Y., Shen, L., Wang, Z. and Ye, K. (2020) Distribution  
734 characteristics and health risks of PAHs in soils and groundwater in typical Karst areas.  
735 *Acta Scientiae Circumstantiae* (in Chinese with English abstract) 40(9), 3361-3374.  
736 Zhu, Y., Tao, S., Price, O.R., Shen, H., Jones, K.C. and Sweetman, A.J. (2015)  
737 Environmental Distributions of Benzo[a]pyrene in China: Current and Future Emission  
738 Reduction Scenarios Explored Using a Spatially Explicit Multimedia Fate Model.  
739 *Environmental Science & Technology* 49(23), 13868-13877.  
740

## Supplementary data for

### Distribution, sources and transport of polycyclic aromatic hydrocarbons (PAHs) in karst spring systems from Western Hubei, Central China

Wei Chen<sup>1,2,3</sup>, Ziqiong Zhang<sup>1</sup>, Ying Zhu<sup>4</sup>, Xianzhen Wang<sup>5</sup>, Longliang Wang<sup>1</sup>, Junwu Xiong<sup>1</sup>, Zhe Qian<sup>1</sup>, Shuai Xiong<sup>2</sup>, Ruichao Zhao<sup>2</sup>, Wei Liu<sup>2\*</sup>, Qiuke Su<sup>6</sup>, Jiangang Zhou<sup>7</sup>, Hong Zhou<sup>2</sup>, Shihua Qi<sup>1</sup>, Kevin C. Jones<sup>8</sup>

1. State Key Laboratory of Biogeology and Environmental Geology, and School of Environmental Studies, and Hubei Key Laboratory of Environmental Water Science in the Yangtze River Basin, and Hubei Provincial Engineering Research Center of Systematic Water Pollution Control, China University of Geosciences, Wuhan 430078, China
2. Institute of Geological Survey, China University of Geosciences, Wuhan 430074, China
3. Ecological Environment Monitoring Station, Ninth Division, Xinjiang Production and Construction Corps, Tacheng, Xinjiang 834601, China
4. School of Environmental Science and Engineering, Shanghai Jiao Tong University, Shanghai 200240, China
5. Geological Exploration Institute of Shandong Zhengyuan, China Metallurgical Geology Bureau, Tai'an 271000, China
6. Nanjing Institute of Environmental Sciences, Ministry of Ecology and Environment, Nanjing 210042, China
7. Geological Exploration Institute of Shandong Zhengyuan, China Metallurgical Geology Bureau, Weifang 261021, China
8. Lancaster Environment Centre, Lancaster University, Lancaster LA1 4YQ, United Kingdom

Corresponding author: Wei Liu, Institute of Geological Survey, China University of Geosciences, Wuhan 430074, China; Email: [wliu@cug.edu.cn](mailto:wliu@cug.edu.cn)

## List of Tables

Table S1. The Chemical Abstracts Service (CAS) number, abbreviation and Method Detection Limits (MDL) of target PAHs in this study.

**P3**

Table S2. Concentrations ( $\text{ng}\cdot\text{L}^{-1}$ ) and detection rate (%) of PAHs in water in the rural karst area in Western Hubei, Central China.

**P4**

Table S3. Concentrations ( $\text{ng}\cdot\text{g}^{-1}$  dw) and detection rate (%) of PAHs in sediment in the rural karst area in Western Hubei, Central China.

**P5**

Table S4. Concentrations ( $\text{ng}\cdot\text{g}^{-1}$  dw) and detection rate (%) of PAHs in soil in the rural karst area in Western Hubei, Central China.

**P6**

Table S5. Rotated principal component matrix of 16 PAHs in the study area.

**P7**

## Lists of Figure

Figure S1. PAHs composition proportion in different environmental medium during the migration process of 9 karst spring systems.

**P8**

**Table S1.** Chemical Abstracts Service (CAS) number, abbreviation, octanol-water partition coefficients (Kow) and method detection limits (MDLs) of target PAHs in this study

PAHs	Abbreviation	CAS. No.	logKow	MDL for liquid samples (ng·L <sup>-1</sup> )	MDL for solid samples (ng·g <sup>-1</sup> )
Naphthalene	Nap	91-20-3	3.37	1.80	0.50
Acenaphthylene	Acy	208-96-8	4.00	0.04	0.10
Acenaphthene	Ace	83-32-9	3.92	0.05	0.05
Fluorene	Flu	86-73-7	4.18	0.04	0.04
Phenanthrene	Phe	85-01-8	4.57	0.13	1.20
Anthracene	Ant	120-12-7	4.54	0.02	0.01
Fluoranthene	Fla	206-44-0	5.22	0.02	0.02
Pyrene	Pyr	129-00-0	5.18	0.05	0.30
Benz( <i>a</i> )anthracene	BaA	1718-53-2	5.91	0.10	0.10
Chrysene	Chry	218-01-9	5.86	0.02	0.05
Benzo( <i>b</i> )fluoranthene	BbF	205-99-2	5.80	0.10	0.06
Benzo( <i>k</i> )fluoranthene	BkF	207-08-9	6.00	0.05	0.10
Benzo( <i>a</i> )pyrene	BaP	50-32-8	6.04	0.20	0.20
Indeno(1,2,3- <i>cd</i> )pyrene	InP	193-39-5	6.50	0.02	0.01
Dibenzo( <i>a,h</i> )anthracene	DahA	13250-98-1	6.75	0.02	0.01
Benzo( <i>ghi</i> )perylene	BghiP	191-24-2	6.50	0.02	0.01

**Table S2.** Concentrations ( $\text{ng}\cdot\text{L}^{-1}$ ) and detection rate (%) of PAHs in water in the rural karst area in Western Hubei, Central China

Compound	Spring water (n=10)				River water (n=10)			
	Range	Median	Mean $\pm$ SD <sup>a</sup>	Detection rate	Range	Median	Mean $\pm$ SD	Detection rate
Nap	2.32-8.15	3.42	4.35 $\pm$ 2.06	100	2.42-9.97	3.29	3.95 $\pm$ 2.10	100
Acy	<MDL-0.80	<MDL	0.17 $\pm$ 0.23	60	<MDL-0.37	0.05	0.10 $\pm$ 0.11	50
Ace	<MDL-0.64	<MDL	0.10 $\pm$ 0.19	20	<MDL-0.24	<MDL	0.05 $\pm$ 0.07	20
Flu	<MDL-4.46	<MDL	0.58 $\pm$ 1.40	40	<MDL-1.29	<MDL	0.15 $\pm$ 0.38	30
Phe	<MDL-40.4	1.38	6.89 $\pm$ 12.7	80	0.06-1.82	0.75	0.76 $\pm$ 0.57	100
Ant	<MDL-4.81	<MDL	0.51 $\pm$ 1.51	30	<MDL-0.01	<MDL	<MDL	10
Fla	<MDL-28.9	<MDL	5.10 $\pm$ 10.5	40	<MDL-0.73	<MDL	0.13 $\pm$ 0.26	10
Pyr	<MDL-161	<MDL	17.9 $\pm$ 50.5	40	<MDL-0.68	<MDL	<MDL	10
BaA	<MDL-0.75	0.43	0.43 $\pm$ 0.19	90	0.34-1.37	0.45	0.53 $\pm$ 0.29	100
Chry	<MDL-0.13	0.05	0.05 $\pm$ 0.04	70	<MDL-0.34	0.02	0.06 $\pm$ 0.11	50
BbF	0.17-2.40	0.37	0.68 $\pm$ 0.70	100	0.21-0.79	0.44	0.45 $\pm$ 0.17	100
BkF	<MDL-0.17	<MDL	<MDL	20	<MDL	<MDL	<MDL	0
BaP	<MDL-1.11	0.28	0.44 $\pm$ 0.36	80	0.24-0.68	0.39	0.41 $\pm$ 0.14	100
InP	<MDL-0.08	<MDL	0.02 $\pm$ 0.02	10	<MDL	<MDL	<MDL	0
DahA	<MDL	<MDL	<MDL	0	<MDL	<MDL	<MDL	0
BghiP	<MDL-0.06	<MDL	0.02 $\pm$ 0.02	20	<MDL	<MDL	<MDL	0
$\Sigma$ LMW-PAHs <sup>b</sup>	3.12-68.8	5.12	17.7 $\pm$ 24.6	100	3.43-10.1	4.55	5.14 $\pm$ 1.93	100
$\Sigma$ HMW-PAHs <sup>c</sup>	0.89-163	1.36	19.6 $\pm$ 51.0	100	1.02-2.92	1.33	1.61 $\pm$ 0.58	100
$\Sigma$ PAHs <sup>d</sup>	4.09-222	6.47	37.3 $\pm$ 69.8	100	4.56-11.4	6.13	6.75 $\pm$ 2.16	100

<sup>a</sup>SD: standard derivation.

<sup>b</sup> $\Sigma$ LMW-PAHs: the total concentrations of low molecular weight PAHs (2-3 ring PAHs).

<sup>c</sup> $\Sigma$ HMW-PAHs: the total concentrations of high molecular weight PAHs (4-6 ring PAHs).

<sup>d</sup> $\Sigma$ PAHs: the total concentrations of 16 PAH compounds.

**Table S3.** Concentrations ( $\text{ng}\cdot\text{g}^{-1}\text{ dw}$ ) and detection rate (%) of PAHs in sediment in the rural karst area in Western Hubei, Central China

Compound	Spring sediment (n=8)				River sediment (n=10)			
	Range	Median	Mean $\pm$ SD <sup>a</sup>	Detection rate	Range	Median	Mean $\pm$ SD	Detection rate
Nap	0.96-8.45	5.43	5.00 $\pm$ 3.05	100	4.86-52.3	9.50	16.6 $\pm$ 15.2	100
Acy	0.12-0.98	0.31	0.38 $\pm$ 0.29	100	0.25-45.0	0.92	8.33 $\pm$ 16.3	100
Ace	0.06-0.29	0.13	0.16 $\pm$ 0.10	100	0.09-11.3	0.22	1.95 $\pm$ 3.96	100
Flu	<MDL-4.70	1.51	1.86 $\pm$ 1.58	87.5	1.71-358	3.60	65.6 $\pm$ 139	100
Phe	1.76—13.5	4.72	6.47 $\pm$ 4.92	100	3.24-332	15.7	65.2 $\pm$ 118	100
Ant	0.01-0.79	0.12	0.23 $\pm$ 0.28	100	<MDL-62.1	0.15	11.4 $\pm$ 24.4	60
Fla	0.74-7.04	1.95	3.15 $\pm$ 2.67	100	0.03-56.1	7.15	12.3 $\pm$ 16.1	100
Pyr	0.51-5.60	1.50	2.48 $\pm$ 2.21	100	0.66-45.6	5.39	10.6 $\pm$ 13.5	100
BaA	<MDL-2.52	0.51	0.88 $\pm$ 0.91	87.5	<MDL-20.5	2.03	4.12 $\pm$ 6.28	90
Chry	0.19-12.7	0.83	2.82 $\pm$ 4.45	100	<MDL-20.9	1.57	3.42 $\pm$ 5.94	90
BbF	<MDL-12.2	0.97	2.88 $\pm$ 4.30	87.5	<MDL-16.6	2.05	3.74 $\pm$ 4.86	90
BkF	<MDL-2.81	0.30	0.68 $\pm$ 0.91	87.5	<MDL-5.78	0.49	1.29 $\pm$ 1.72	90
BaP	0.23-4.35	0.66	1.35 $\pm$ 1.41	100	<MDL-9.14	0.89	2.08 $\pm$ 3.00	90
InP	<MDL-3.88	0.05	0.83 $\pm$ 1.39	87.5	<MDL-8.87	0.01	1.07 $\pm$ 2.65	50
DahA	<MDL-1.10	0.01	0.23 $\pm$ 0.42	62.5	<MDL-0.15	<MDL	0.02 $\pm$ 0.04	20
BghiP	<MDL-4.87	<MDL	0.96 $\pm$ 1.74	37.5	<MDL-1.66	<MDL	0.16 $\pm$ 0.50	50
$\Sigma$ LMW-PAHs <sup>b</sup>	4.34-34.2	16.5	17.3 $\pm$ 11.9	100	13.7-913	43.0	181 $\pm$ 330	100
$\Sigma$ HMW-PAHs <sup>c</sup>	1.53-48.7	6.95	13.1 $\pm$ 16.1	100	2.59-128	13.1	26.4 $\pm$ 37.2	100
$\Sigma$ PAHs <sup>d</sup>	5.87-83.0	23.8	30.3 $\pm$ 25.9	100	29.9-1041	57.2	227 $\pm$ 379	100

<sup>a</sup>SD: standard derivation.

<sup>b</sup> $\Sigma$ LMW-PAHs: the total concentrations of low molecular weight PAHs (2-3 ring PAHs).

<sup>c</sup> $\Sigma$ HMW-PAHs: the total concentrations of high molecular weight PAHs (4-6 ring PAHs).

<sup>d</sup> $\Sigma$ PAHs: the total concentrations of 16 PAH compounds.

**Table S4.** Concentrations ( $\text{ng}\cdot\text{g}^{-1}$  dw) and detection rate (%) of PAHs in surface soil in the rural karst area in Western Hubei, Central China

Compound	Soil (n=9)			Detection rate
	Range	Median	Mean $\pm$ SD <sup>a</sup>	
Nap	0.94-13.2	4.32	4.54 $\pm$ 3.85	100
Acy	0.14-1.06	0.32	0.42 $\pm$ 0.31	100
Ace	<MDL-0.46	0.17	0.21 $\pm$ 0.13	88.9
Flu	<MDL-2.87	0.88	0.99 $\pm$ 0.87	88.9
Phe	1.32-7.13	3.83	4.03 $\pm$ 2.18	100
Ant	<MDL-0.02	<MDL	0.01 $\pm$ 0.01	44.4
Fla	<MDL-8.47	1.76	2.73 $\pm$ 3.03	88.9
Pyr	0.50-7.79	1.42	2.54 $\pm$ 2.70	100
BaA	0.21-4.61	0.68	1.53 $\pm$ 1.91	100
Chry	0.33-4.96	1.16	1.72 $\pm$ 1.49	100
BbF	<MDL-8.22	1.06	2.13 $\pm$ 2.84	88.9
BkF	0.22-2.44	0.89	0.99 $\pm$ 0.76	100
BaP	0.21-5.03	0.85	1.31 $\pm$ 1.55	100
InP	<MDL-9.77	0.02	1.32 $\pm$ 3.42	66.7
DahA	<MDL-1.41	0.01	0.20 $\pm$ 0.49	55.6
BghiP	<MDL-8.86	0.02	1.13 $\pm$ 3.12	55.6
$\Sigma$ HMW-PAHs <sup>b</sup>	1.98-51.0	6.11	12.8 $\pm$ 16.6	100
$\Sigma$ LMW-PAHs <sup>c</sup>	3.74-26.0	11.3	12.9 $\pm$ 8.15	100
$\Sigma$ PAHs <sup>d</sup>	6.04-67.7	18.1	25.8 $\pm$ 21.2	100

<sup>a</sup>SD: standard derivation.

<sup>b</sup> $\Sigma$ LMW-PAHs: the total concentrations of low molecular weight PAHs (2-3 ring PAHs).

<sup>c</sup> $\Sigma$ HMW-PAHs: the total concentrations of high molecular weight PAHs (4-6 ring PAHs).

<sup>d</sup> $\Sigma$ PAHs: the total concentrations of 16 PAH compounds

**Table S5.** Rotated principal component matrix of 16 PAHs in the study area

PAHs	Ring	Principal component			
		Factor 1	Factor 2	Factor 3	Factor 4
Nap	2	0.052	<b>0.798</b>	0.173	-0.238
Acy	2	<b>0.622</b>	0.421	0.545	-0.068
Ace	2	-0.043	-0.009	-0.015	<b>0.933</b>
Flu	2	0.264	<b>0.948</b>	0.009	-0.065
Phe	3	0.102	<b>0.887</b>	0.372	0.114
Ant	3	0.222	<b>0.787</b>	0.197	0.295
Fla	3	0.18	0.378	<b>0.892</b>	-0.051
Pyr	4	0.234	0.301	<b>0.91</b>	0.08
BaA	4	0.459	-0.045	<b>0.861</b>	-0.022
Chry	4	<b>0.762</b>	0.517	0.084	0.268
BbF	4	<b>0.83</b>	0.407	0.244	0.102
BkF	4	<b>0.835</b>	0.162	0.199	0.345
BaP	5	<b>0.932</b>	0.121	0.208	0.004
InP	5	<b>0.908</b>	-0.03	0.276	-0.2
DaA	5	<b>0.96</b>	0.199	0.133	-0.085
BgP	6	<b>0.939</b>	0.067	0.24	-0.144
Variance/ %		38.4	32.6	28.1	0.9
Estimated source	/	Coal combustion and vehicle emission sources	Biomass combustion source	Coal combustion source	Petrogenic source

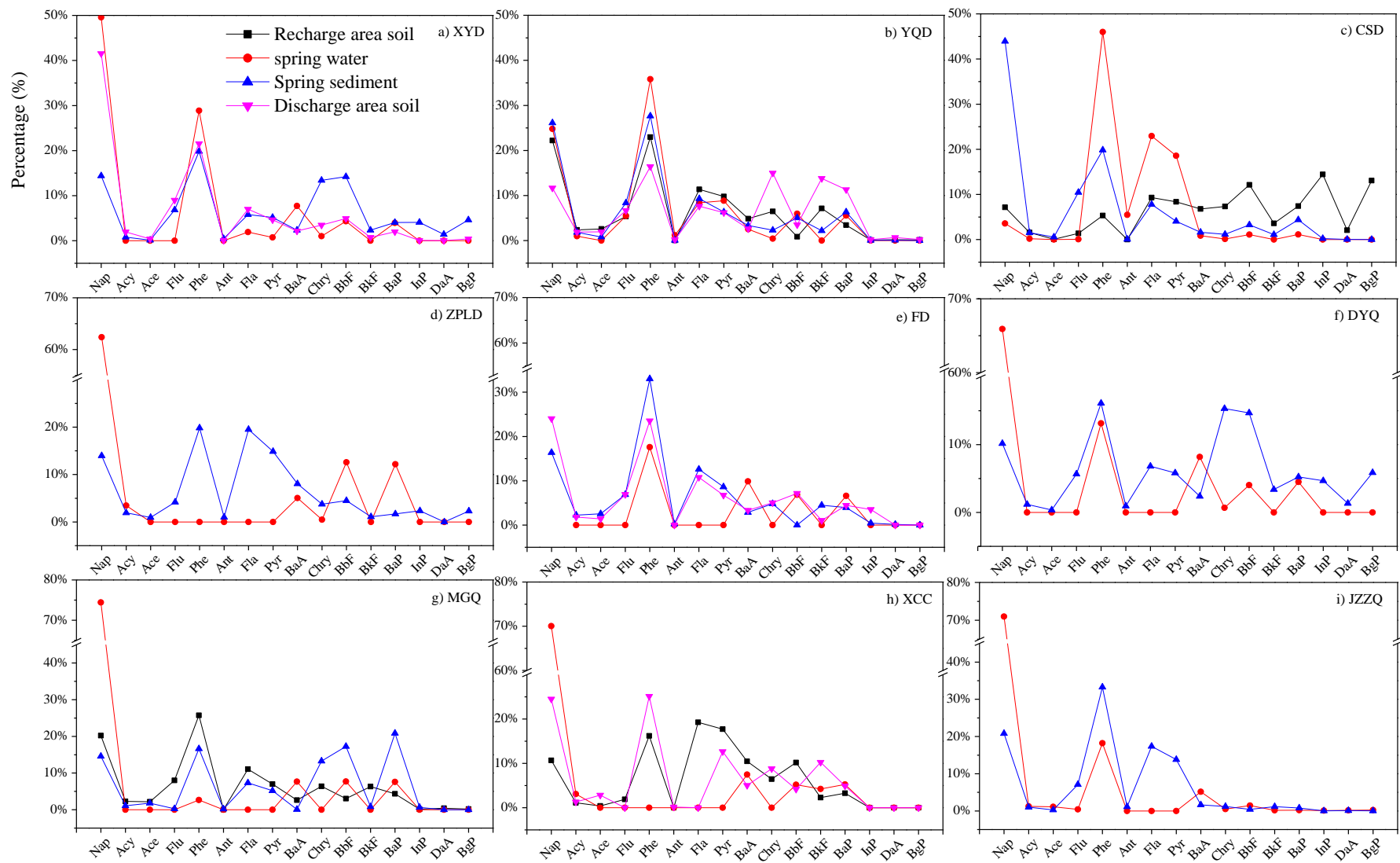


Fig. S1. PAHs compositions in different environmental medium during the migration process of 9 karst spring systems